# Considering Mine Countermeasures Exploratory Operations Conducted By Autonomous Underwater Vehicles

BAO NGUYEN[1, 2], DAVID HOPKIN[2], and HANDSON YIP[3]

[1]Defence Research and Development Canada – Centre for Operational Research and Analysis

[2]Defence Research and Development Canada – Atlantic

[3]Allied Command Transformation, Staff Element Europe, Capability Goals & Standards

Recent improvements in Autonomous Underwater Vehicle (AUV) technology are making AUVs increasingly attractive as mine-hunting platforms by extending the reach of the sensors and weapons used in such operations. In this paper, we describe novel concepts of operations for AUVs performing Mine Countermeasures (MCM) exploratory operations. These concepts maximize MCM effectiveness and minimize resources in such operations. In particular, this paper describes how previously unmodeled characteristics, such as the aspect and range dependencies of mine detection, have a significant influence on the mission effectiveness of a side-scan sonar, specifically one that is typical of the experimental Remote Mine-Hunting System (RMS) developed by Defence Research and Development Canada – Atlantic. Note that a nontechnical version of this paper has appeared in Nguyen et al (2008).

# BACKGROUND

The availability of affordable commercial-off-the-shelf (COTS) Autonomous Underwater Vehicles (AUVs) equipped with side-scan sonar is beginning to transform the way detection is conducted in Mine Countermeasures (MCM) operations. These AUVs can achieve higher efficiency and effectiveness than can conventional assets, at near zero risk to human life. Cost-effective, lightweight COTS AUVs are also particularly favored by the military community because of their minimal logistical requirements for rapid deployment and handling.

A frequent and important MCM operation is the "MCM exploratory operation" (also known as an "MCM reconnaissance operation"). The aim of an MCM exploratory operation is to determine the presence or absence of mines in an area of operation. If a mine is detected, classified, and identified during an MCM exploratory operation, then the naval commander will consider another route or a mine clearance operation will follow. In both cases, there will be expensive costs. For instance, a mine clearance operation is often very time-consuming due to a number of environmental factors such as cluttered seabeds, low underwater visibility, strong tidal currents and unfavorable sea states. In addition, an exploratory search aims to find the first mine. Therefore an MCM exploratory operation is essential before a clearance operation as an MCM operation reduces search time considerably. It is also an essential step before deploying any high-value asset in potentially mined waters.

The use of AUVs in MCM exploratory operations is relatively recent; therefore, there is a lack of knowledge on how to employ them efficiently and effectively. In this paper, we will focus on two key metrics that characterize the efficiency and effectiveness of AUVs in such operations. The first metric is the confidence that mines are or are not present in the search area. The second metric is the time required to achieve that confidence level.

Any search strategy must take into account the current mindset and operating practices of the operator, as well as the technological constraints of today's AUV systems. The preferred way to conduct an exploratory search of a large area is to segment the area into smaller areas that can be searched in a series of short missions. Typically, the operator would plan each AUV mission such that the AUV would bring back data for analysis within a few hours. In this experiment, the trial area has been partitioned into sixteen 3 km × 3 km square cells, as shown in Fig. 1. Table 1 summarizes the parameters defining the scenario and the capabilities of the *Dorado,* the AUV developed by Defence Research and Development Canada (DRDC) – Atlantic, depicted in Fig. 2.

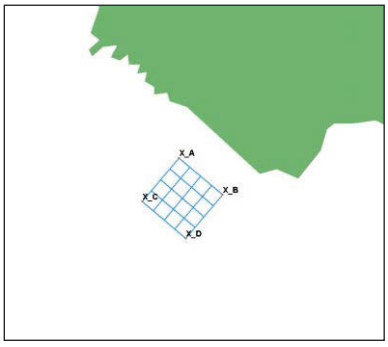


Figure 1. Search areas (gulf of La Spezia, Italy).

Table 1 – Scenario parameters.

| *Parameter* | *Value* |
|---|---|
| Total Area: 16 Segmented Areas | 12 km × 12 km |
| Segmented Area | 3 km × 3 km |
| AUV Speed | 9 knots |
| AUV Endurance | 30 hours |

Figure 2. The *Dorado.*

## ASSUMPTIONS

In this paper, we assume that the AUV carries a side-scan sonar. The mine-hunting

environment plays an important role in the performance of side-scan sonar, as it does for any MCM sensor. Seabed conditions such as clutter, composition, and topology have the most significant effects on the sensor's detection performance. However, in this first attempt to analyze the effectiveness of AUVs, we assume benign seabed conditions with high-target-strength mines. Such circumstances allow reasonable assumptions to be made about sensor performance. Specifically, the probability of identifying a mine as a mine is very high (approximately 100 percent) while the probability of identifying a non-mine as a mine is very low (approximately 0 percent).

The interior of the rectangular frame in Fig. 3 is the search area, within which solid lines represent the AUV path while circles indicate mines. The arrow in the search area indicates the general direction of the AUV's transit. The vehicle starts at the bottom left, travels from left to right, travels upward, travels from right to left, and then travels upward and repeats this motion.

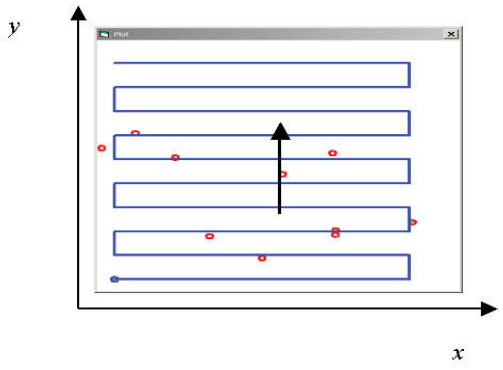


Figure 3. Coordinate system.

The AUV path shown in Fig. 3 is a typical search pattern called the "lawn-mowing pattern" or the "parallel search pattern." This and every search pattern is characterized by its resulting measures of effectiveness (MOEs). These MOEs may include probability of detection, coverage, overlap, and search time. They can be determined using the scenario's geometry and the sonar's measures of performance (MOPs).

## MEASURES OF PERFORMANCE

Side-scan sonars are high resolution sensors that typically collect images of the seabed. These images are then analyzed either by a human operator or by software. One criterion to detect a mine is to measure the size of its shadow. On the left-hand side (LHS) of Fig. 4, a mine is observed at an angle of 85 deg and would without a doubt be identified by an experienced operator (based on the shadow). On the right-hand side (RHS) of Fig. 4, the same mine is observed at an angle of 0 deg, and is not recognizable at all.

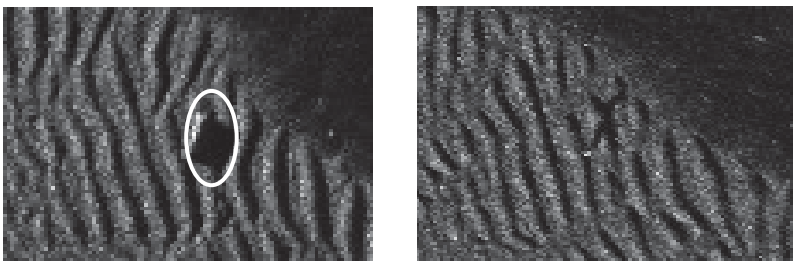

Figure 4. Mine observed at 85 deg (LHS) and at 0 deg (RHS).

Generally, at a given range, it is approximately true that the size of the shadow of a thin cylindrical mine is maximal when the mine's aspect angle is perpendicular to the side-

scan sonar beam, and decreases symmetrically as the angle deviates from the perpendicular case. The aspect angle is defined as the angle between the sonar beam and the axis of symmetry of a cylindrical mine. To identify the shadow of a mine, it is also necessary that the mine lies between the minimum range and the maximum range of detection. The range corresponds to the distance between the AUV and a target at the closest point of approach.

The information above allows us to model the sonar's measures of performance (MOPs): the probability of detection as a function of range, as shown on the LHS of Fig. 5, and the probability of detection as a function of aspect angle, as shown on the RHS of Fig. 5.

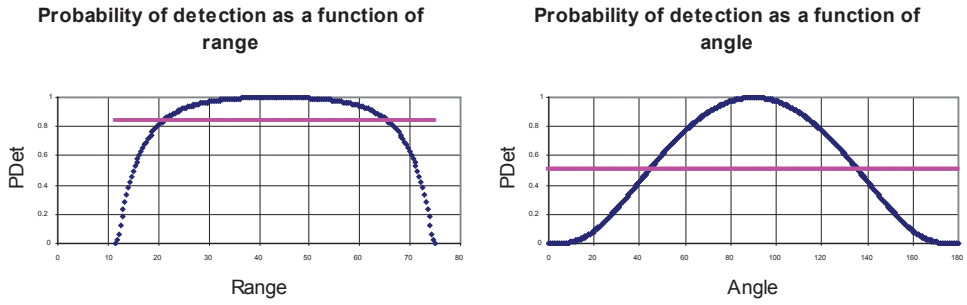


Figure 5. Probability of detection as a function of range (LHS) and angle (RHS).

The range probability curve implies that if a mine lies between the minimum range and the maximum range, then it will be detected with a probability close to 100 percent. We refer to the minimum range as the gap in coverage in the sense that if a mine lies between the sonar and its minimum detection range then it will not be detected. The angular probability curve implies that probability of detection of the mine reaches a maximum

when the mine's aspect angle is perpendicular to the side-scan sonar beam, and decreases symmetrically as the angle deviates from the perpendicular case. It is clear from Fig. 5 that the probability of detection is substantially degraded if the aspect angle differs from 90 deg. The impact of this degradation is shown in Fig 4. Data and models supporting these properties can be found in Couillard et al 2007, Fawcett et al 2006, Fawcett et al 2008, Hill et al 2006 and Quidu et al 2001.

Probability of detection as a function of range represents a characteristic of the side-scan sonar, while probability of detection as a function of angle represents a characteristic of the mine. These probability curves are modelled using the Johnson distribution. Eq. (1) (Law et al 2000) is parameterized using the values in Table 2. The scale ($\lambda$) shown below is a factor compounded to Johnson's distribution such that the maximal value of each curve is equal to 1.

Johnson's curve can be expressed as:

$$f(x) = f_J(x) = \begin{cases} \dfrac{\lambda \cdot \alpha_2 \cdot (x_2 - x_1)}{(x - x_1) \cdot (x_2 - x) \cdot \sqrt{2\pi}} e^{-\frac{1}{2}\left(\alpha_1 + \alpha_2 \cdot \ln\left(\frac{x - x_1}{x_2 - x}\right)\right)^2} & x_1 < x < x_2 \\ 0 & \text{otherwise} \end{cases} \quad (1)$$

Johnson's distribution curves are used because they are flexible and convenient for modeling. By choosing the parameters that define Johnson's curves, we can simulate a number of behaviors: we can choose the minimum and the maximum value of the

variable, and we can make it unimodal or bimodal, skewed to the left, symmetric, or skewed to the right as well as controlling how narrow each peak is.

Table 2 – Johnson parameters defining the range and angle probability curves.

| | *Johnson's Parameters* | |
|---|---|---|
| Range Probability Curve | $\alpha_1 = 0\,,\ \alpha_2 = 0.75$ | $x_1 = 11.5\ \text{m}\,,\ x_2 = 75\ \text{m}$ |
| Angular Probability Curve | $\alpha_1 = 0\,,\ \alpha_2 = 1.25$ | $x_1 = 0\,,\ x_2 = \pi$ |

As discussed above, the shape and the symmetry of the angular probability of detection is essentially independent of the range probability of detection. Therefore, we approximate the resulting probability of detection as $P(D \mid r,\theta) = f_R(r) \cdot f_\Theta(\theta)$ where $D$ stands for detection; $r$ stands for range and $f_R(r)$ is the range probability of detection; $\theta$ stands for aspect angle and $f_\Theta(\theta)$ is the angular probability of detection. For brevity, we will suppress the symbol $D$ in the paper.

## PRELIMINARY RESULTS

If we assume that the spacing between two consecutive horizontal legs of the lawn-mowing search pattern shown in Fig. 3 is typically equal to twice the maximum range of detection, then there is no overlap in coverage between two consecutive horizontal legs and the probability of detection obtained by the lawn-mowing search pattern is approximately 40 percent. We arrive at this figure by noting that the mean range probability of detection is about 80 percent (LHS of Fig. 5) while the mean angular

probability of detection is about 50 percent (RHS of Fig. 5). Thus, the final probability is the product, or 40 percent.

The usual lawn-mowing pattern poses two problems. First, the MOEs are affected by the gap in detection range. Second, there is a substantial degradation in the probability of detection due to angular effects. The next section presents solutions to these problems.

## CONCEPTS OF OPERATIONS

Gaps in Coverage. If the AUV conducts an uneven lawn-mowing pattern, as shown in Fig. 6, then it will eliminate gaps in coverage. This search pattern is designed to provide 100 percent coverage of the search area, in addition to minimizing overlaps and search time with respect to other mowing paths. With that in mind, we derive that the small spacing between horizontal legs must be equal to the maximum detection range minus the minimum detection range $(r_{\max} - r_{\min})$, while the large spacing between them must be equal to twice the maximum detection range $(2 \cdot r_{\max})$. Note that this solution can be fulfilled only if $r_{\max} \geq 3 \cdot r_{\min}$, a condition that is met by the parameters shown in Table 2. There are an advantage and a disadvantage to the uneven lawn mowing search pattern. The advantage is that there is no gap hence improving the probability of detection. The disadvantage is that it takes more time to conduct an uneven lawn mowing search pattern than to conduct an even lawn mowing search pattern. To choose one over another depends on the priority of the mission.

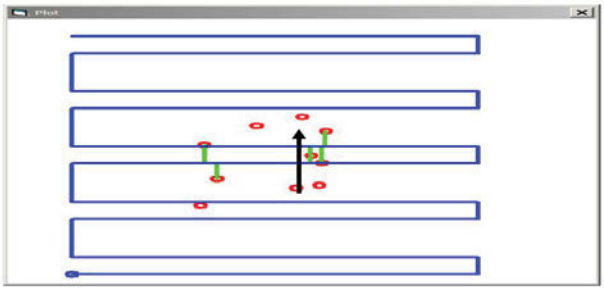

Figure 6. Uneven lawn-mowing pattern.

Aspect Angle Degradation. Degradation due to angular probability of detection, described in the previous section, can be mitigated by fusing more than one observation of a mine at different aspect angles (Nguyen and Hopkin 2005 a & b, and Zerr et al 2000). Assume a cylindrical mine is observed from two angles: 30 deg and 60 deg. Note that to achieve two looks at 30 deg and 60 deg, we make use of three lawn mowing search patterns that are offset by 60 deg with respect to one another. This will be further discussed in the "Optimality with N Different Angular Observations" section. The fusion of these two observations improves the angular probability of detection by six percentage points based on the probability curve shown on the RHS of Fig. 5. We can understand this improvement by observing that the angular probability of detection by the first AUV leg is $P_1 = 77$ percent while the angular probability of detection by the second AUV leg is equal to $P_2 = 24$ percent. Combining the results of the two AUV legs, the angular probability of detection becomes $P_{1-2} = 1-(1-P_1)(1-P_2) = 83$ percent – an improvement of six percentage points with respect to $P_1 = 77$ percent. We assume this is a stochastic process. Hence, looking at a mine from a different aspect angle improves the probability

of detection generally. More often than not, the seabed will also help differentiate the observation from one aspect angle to another (see Fig. 4).

## Optimality with Two Different Angular Observations

If the AUV can observe the same mine from two different angles, then it is natural to ask how the two angles should be related to one another such that the angular probability of detection is optimal. We define $P_1$ to be the mean angular probability of detection generated by one AUV leg while $P_2(\phi)$ to be the mean angular probability of detection generated by two AUV legs, calculated as a function of the angle $\phi$ between them. $P_2(\phi)$ achieves a maximum when $\phi = 90\ \text{deg}\left(\frac{\pi}{2}\right)$. That is, to maximize the angular probability of detection with two observations at different angles, the difference between the angles must be $90\ \text{deg}\left(\frac{\pi}{2}\right)$.

The proof of this assertion is described below. However, for the purpose of this section, it is convenient to redefine the aspect angle $\theta$ by rotating it to the left by 90 deg such that the maximum angular probability of detection occurs at 0 deg.

To obtain $P_1$ and $P_2$, we assume that a mine lies between the minimum and maximum range of an AUV leg and two AUV legs, respectively. We compute $P_1$ by integrating the angular probability of detection, shown on the LHS of Fig. 5, from $-90\ \text{deg}\left(-\frac{\pi}{2}\right)$ to

$+90\deg\left(\frac{\pi}{2}\right)$ and then averaging it through a division by $180\deg(\pi)$. We compute $P_2$ in the same way, except that it is based on two AUV legs whose relative angle is $\phi$.

$$P_1 = \frac{1}{\pi} \cdot \int_{-\frac{\pi}{2}}^{\frac{\pi}{2}} d\theta \cdot f(\theta) \tag{2}$$

$$P_2(\phi) = 1 - \frac{1}{\pi} \cdot \int_{-\frac{\pi}{2}}^{\frac{\pi}{2}} d\theta \cdot \left(1 - f(\theta)\right) \cdot \left(1 - f(\theta + \phi)\right) \tag{3}$$

Here, $f(\theta)$ is the Johnson function whose parameters are defined in Table 2. The fact that $P_2$ reaches a maximum at $\phi = 90\deg\left(\frac{\pi}{2}\right)$ is true in general. It is due to the shape and symmetry of the angular probability of detection curve. Observe that the derivative of $P_2(\phi)$ at $\phi = 90\deg\left(\frac{\pi}{2}\right)$ is:

$$\frac{d}{d\phi} P_2(\phi)\Big]_{\phi=\frac{\pi}{2}} = \frac{1}{\pi} \cdot \int_{-\frac{\pi}{2}}^{\frac{\pi}{2}} d\theta \cdot \left(1 - f(\theta)\right) \cdot \frac{d}{d\phi} f(\theta + \phi)\Big]_{\phi=\frac{\pi}{2}} \tag{4}$$

Since $f(\theta)$ is an even function of $\theta$, $1 - f(\theta)$ is also an even function of $\theta$. In addition, $\frac{d}{d\phi} f(\theta + \phi)\Big]_{\phi=\frac{\pi}{2}}$ is an odd function of $\theta$. Hence, the integrand of Eq. (4) is odd at $\phi = 90\deg\left(\frac{\pi}{2}\right)$, implying that $\frac{d}{d\phi} P_2(\phi)\Big]_{\phi=\frac{\pi}{2}} = 0$. Therefore, $P_2(\phi)$ achieves an optimum at

$\phi = 90\ \text{deg}\left(\frac{\pi}{2}\right)$. Appendix A further shows that this is not merely an optimum but in fact a global maximum. Based on the parameters shown in Table 2, we get $P_1 = 0.50$ and $P_2\left(\phi = \frac{\pi}{2}\right) = 0.88$.

Optimality with N Different Angular Observations

It turns out that we can generalize the result in the previous subsection. That is, we are able to determine the angles such that the angular probability of detection is optimal when a mine is observed $N$ times from the same range. We show that if $\phi_i = i \cdot \varphi$ where $i = 0..N-1$ and $\varphi = \frac{\pi}{N}$, then the resulting mean angular probability of detection is maximal. For example, if there are three angular observations, then the mean angular probability of detection is maximal when $\phi_0 = 0; \phi_1 = \pi/3; \phi_2 = 2\pi/3$.

To prove this assertion, we only need to show that $\left(\frac{\partial}{\partial \phi_0} P_N\left(\vec{\phi}\right)\right)_{\phi_i = i\cdot\theta} = 0$, since we can always choose a coordinate system that is rotated in such a way that for any $i$, $\phi_i$ becomes zero. Note that $\left(\frac{\partial}{\partial \phi_0} P_N\left(\vec{\phi}\right)\right)_{\phi_i = i\cdot\theta}$ can be expressed as:

$$\left(\frac{\partial}{\partial \phi_0} P_N\left(\vec{\phi}\right)\right)_{\phi_i = i\cdot\theta} = \int_{-\frac{\pi}{2}}^{\frac{\pi}{2}} \frac{d\theta}{\pi} \cdot g'(\theta) \cdot g(\theta + \varphi) \cdot \ldots \cdot g\left(\theta + (N-1)\cdot\varphi\right) \tag{5}$$

The above is zero if $g'(\theta)$ is odd and $g(\theta+\varphi)\cdot g(\theta+2\cdot\varphi)\cdot\ldots\cdot g(\theta+(N-1)\cdot\varphi)$ is even, as this implies that the integrand is odd, and integrating an odd function from $-\pi/2$ to $\pi/2$ gives zero.

Since $g(\theta)$ is even, we infer that $g'(\theta)$ is odd. Moreover,

$$
\begin{aligned}
&g(-\theta+\varphi)\cdot g(-\theta+2\cdot\varphi)\cdot\ldots\cdot g(-\theta+(N-1)\cdot\varphi)\\
&=g(\theta-\varphi)\cdot g(\theta-2\cdot\varphi)\cdot\ldots\cdot g(\theta-(N-1)\cdot\varphi)\\
&=g(\theta-\varphi+N\cdot\varphi)\cdot g(\theta-2\cdot\varphi+N\cdot\varphi)\cdot\ldots\cdot g(\theta-(N-1)\cdot\varphi+N\cdot\varphi)\\
&=g(\theta+(N-1)\cdot\varphi)\cdot g(\theta+(N-2)\cdot\varphi)\cdot\ldots\cdot g(\theta+\varphi)
\end{aligned}
$$

The first equality is true due to the fact that $g(\theta)$ is even. The second equality is true due to the fact that $g(\theta)$ is periodic with a period equal to $N\cdot\varphi=\pi$. The last equality shows that the product is an even function. Hence the integrand of Eq. (5) is odd and thus the integral is zero. In practice, given the angular measure of performance, we can determine the number of optimal looks such that the angular probability of detection meets a desired threshold. Again, the above proof does not require the exact values of $g(\theta)$ but only its shape and symmetry. There is evidence in the literature such as Bays et al 2011 where an area of interest is searched using a star search pattern to maximize the overall probability of detection. In this context, a star search pattern is a pattern that is composed of straight legs whose angular orientations are offset by 60 degrees with respect to one another. On the one hand, employing a multiple look search pattern such as the star search pattern generates overlaps which increases the search time. On the other hand, the overlaps will significantly improve the probability of detecting a mine and thus offer a higher

probability of detection to naval undersea warfare commanders. This agrees with Hill et al 2006 where search tactics that involved overlaps improved the probability of detection.

## MODELLING AND ALGORITHMS

Now that we have found a solution that eliminates gaps in coverage and mitigates degradation in probability of detection due to aspect angle, we shall implement this solution in a Monte Carlo model and a deterministic model. The Monte Carlo model is coded in Visual Basic (VB) while the deterministic one is coded in Mathcad. The two are distinct but equivalent. They allow validation of the MOEs by comparing those from the Monte Carlo simulation to those obtained by the deterministic model.

*Monte Carlo Simulation*. For each run, the AUV employs the same search path, while the mines' positions and angles are generated using an *a priori* distribution. The simulation then computes the probability of detection using the range probability curve and the angular probability curve. It also fuses data when the same mine is detected by multiple legs and/or multiple AUVs. The program collects the results of each run, performs the statistics, and outputs the MOEs.

We make use of the Chernoff bound (Vidyasagar 1998) to determine the number of Monte Carlo runs $(m)$ required to achieve a given accuracy $(\varepsilon)$ and a predetermined confidence level $(1-\delta)$:

$$m \geq \frac{1}{2 \cdot \varepsilon^2} \cdot \ln\left(\frac{2}{\delta}\right)$$

This criterion implies that:

$$P\left(\left|\hat{P} - P_T\right| \leq \varepsilon\right) = 1 - \delta$$

where $\hat{P}$ is the estimated probability collected from the Monte Carlo simulation of $m$ runs while $P_T$ is the true probability. As an example, to meet a 5 percent accuracy $(\varepsilon = 0.05)$ and a 95 percent $(\delta = 0.05)$ confidence level, we need 738 runs. Note that another way to determine the number of runs is to make use of the central limit theorem (Zwillinger 1996) where $m = \left(z_{\delta/2} \cdot \left(\frac{\sigma}{\varepsilon}\right)\right)^2$; $z_{\delta/2} = 1.96$ at 95 percent confidence level, $\varepsilon = 0.05$ and $\sigma$ is the standard deviation. Since $\hat{p}$ is a probability its standard deviation $\sigma$ must be less than or equal to $0.5$. Hence, $m$ is roughly equal to $400$ runs for a $5$ percent accuracy and a 95 percent confidence level. We observe that the number of runs based on the central limit theorem is smaller than the one based on the Chernoff bound. This confirms the validity of the Chernoff bound. An advantage to the Chernoff bound is that we do not need to know $\sigma$ to determine the number of runs.

*Deterministic Model*. We divide the search area into 200-by-200 grid of cells. For each leg of the AUV's sweep, we look at each cell and determine whether it lies between the

AUV's minimum and maximum detection ranges. If it does, then we compute the probability of detection using the probability curves and the probability density of the mines.

For example, if the mines are uniformly random over the entire search area, then the probability density of a cell is equal to the area of the cell divided by the size of the search area. The corresponding contribution of each cell to the total probability of detection is simply equal to $\left(\Delta \cdot P_g / A\right)$, where $A$ is the size of the search area, $\Delta$ is the size of the cell, and $P_g$ is the probability of detection of that cell based on range, aspect angle, and the AUV's search path. The probability $P_g$ can be expressed as $P_g = 1 - \prod_{i=1}^{d} (M_i)$, where $d$ is the number of AUV legs whose coverage contains that cell and $M_i (\leq 1)$ is the probability that the i$^{th}$ leg misses the same cell. In general, as $d$ increases, so does $P_g$.

In Nguyen et al 2008, we determine the probability of detection, based on the Monte Carlo simulation and the deterministic calculation, and demonstrate that our calculations are consistent, because the two models, despite being designed differently, provide the same statistical result. However, this Monte Carlo simulation offers more flexibility. For example, we can use the simulation to model the details of the seabed. We will be enhancing the simulation with this feature and will report the results in a future paper.

## Random Search Formula Adapted to AUVs

Before we present the results of the models described above, we will derive a formula for the probability of detection of an AUV conducting a random search. This formula will allow comparisons of effectiveness between a random search and the novel concepts of operations proposed for AUVs. Since the side-scan sonar MOPs (Fig. 5) indicate that the detection probability is not perfect in general, and in fact depends on both range and angle, it is clear that we need to modify Koopman's formula (Koopman 1999) to determine the detection probability of an AUV conducting random search operations. Fortunately, this modification is simple, so we will present the derivation below.

This derivation is based on similar assumptions as those made for Koopman's random search. That is, (Koopman 1999):

a. The target's position is uniformly distributed in the search area i.e. the density distribution is equal to $1/A$ where $A$ is the size of the search area;
b. The AUV's path is random in $A$ in the sense that it can be thought of as having its different portions placed independently of one another in $A$.
c. On any portion of the path that is small relative to the total length of path but decidedly larger than the range of possible detection, the AUV always detects the target that lies between the maximal range $r_{\max}$ and the minimal range $r_{\min}$ on either side of the path and never beyond.

Using the above assumptions, we divide the search length $L$ into $n$ search segments, each with length $L/n$. The maximum detection range $r_{\max}$, the minimum detection range $r_{\min}$, and the length of each segment cover two small rectangles. We assume that these rectangles lie inside the search area. Based on the uniform density distribution, the probability of detection of a mine lying in this subarea is equal to:

$$p_K(\theta) = \frac{L}{n} \cdot \frac{2 \cdot \int_{r_{\min}}^{r_{\max}} p_R(r) \cdot dr}{A} \cdot p_\Theta(\theta) \tag{6}$$

where $p_R(r)$ is the detection probability as a function of range $(r)$, as shown on the LHS of Fig. 5, while $p_\Theta(\theta)$ is the detection probability as a function of angle $(\theta)$, as shown on the RHS of Fig. 5. (The $K$ stands for Koopman.) In a random search, this angle $\theta$ is uniformly random because the mine's orientation is random, which is equivalent to the AUV changing course randomly relative to a mine of fixed orientation. Eq. (6) can be further simplified by recalling that the detection probability as a function of range was modeled as a Johnson density distribution scaled by $\lambda_r$ as defined in Eq. (1):

$$\int_{r_{\min}}^{r_{\max}} p_R(r) \cdot dr = \int_{r_{\min}}^{r_{\max}} f(r) \cdot dr = \lambda_r \cdot \int_{r_{\min}}^{r_{\max}} f_J(r) \cdot dr = \lambda_r$$

The probability that a mine lies in the subarea can now be written as:

$$p_K(\theta) = \frac{(L/n) \cdot 2 \cdot \lambda_r}{A} \cdot p_\Theta(\theta) \tag{7}$$

The probability that a mine lies outside of this rectangle is simply:

$$q_K(\theta) = 1 - p_K(\theta) \tag{8}$$

The only way that the AUV misses a mine after *n* independent and random search segments is to miss it in every search segment. As a result, the detection probability due to *n* search segments is equal to:

$$P_K = 1 - \prod_{i=1}^{n}\left(q_K(\theta_i)\right) = 1 - \prod_{i=1}^{n}\left(1 - \frac{2 \cdot \lambda_r \cdot (L/n)}{A} \cdot p_\Theta(\theta_i)\right) \tag{9}$$

Expanding the product:

$$\begin{aligned} P_K &= 1 - \left(1 - \frac{L \cdot 2 \cdot \lambda_r}{n \cdot A} \cdot \sum_{i=1}^{n} p_\Theta(\theta_i) + \ldots\right) \\ &= 1 - \left(1 - \frac{L \cdot 2 \cdot \lambda_r}{A \cdot \pi} \cdot \frac{\pi}{n} \sum_{i=1}^{n} p_\Theta(\theta_i) + \ldots\right) \\ &= 1 - \left(1 - \frac{L \cdot 2 \cdot \lambda_r}{A \cdot \pi} \cdot \int_0^\pi d\theta \cdot p_\Theta(\theta) + \ldots\right) \end{aligned} \tag{10}$$

The key argument in Eq. (10) is the third equality. The sum in the second equality when compounded to $\frac{\pi}{n}$ is exactly $\int_0^\pi p_\Theta(\theta) \cdot d\theta$. This is a Monte Carlo integration when *n* is large (Press et al 1992). Again, recalling that $p_\Theta(\theta)$ was modeled as a Johnson's density distribution scaled by $\lambda_\theta$, we get $\int_0^\pi p_\Theta(\theta) \cdot d\theta = \lambda_\theta$. Taking the limit as *n* tends to infinity yields the following formula (Zwillinger 1996):

$$
\begin{aligned}
P_K &= 1-\left(1-\frac{L\cdot 2\cdot \lambda_r\cdot \lambda_\theta}{A\cdot \pi}+\ldots\right) \\
&= 1-\left(1-\frac{L\cdot 2\cdot \lambda_r\cdot \lambda_\theta}{n\cdot A\cdot \pi}\right)^n \\
&= 1-e^{-\left(\frac{2\cdot \lambda_r\cdot L}{A}\cdot\frac{\lambda_\theta}{\pi}\right)} \\
&= 1-e^{-\left(\frac{2\cdot \lambda_r\cdot V\cdot t}{A}\cdot\frac{\lambda_\theta}{\pi}\right)}
\end{aligned}
\tag{11}
$$

Here, $P_K$ is the probability of an AUV detecting a mine while conducting a random search at velocity *V* for time *t.* This formula has an attractive interpretation. The detection range *R* is replaced by an effective range $R_{effective}=\lambda_r$ due to two characteristics of the probability of detection as a function of range. First, there is a minimum detection range; i.e., if a mine is observed at a range less than the minimum detection range, then it will not be detected. Second, detection is not perfect for a mine lying between the minimum and maximum ranges. Hence, the original detection range is replaced by an effective detection parameter $\lambda_r$. For example, in our scenario the minimum detection range is 11.5 m while the maximum detection range is 75.0 m. This generates an effective detection range $\lambda_r$ of approximately 53.06 m.

Additionally, the exponential's power includes a factor of $\frac{\lambda_\theta}{\pi}$, which represents the mean angular probability of detection. In our scenario, the effective angular range, $\lambda_\theta$, is approximately 90 deg, implying a mean angular detection probability of approximately 50 percent. This modification is essential, as Koopman's original formula assumes no

angular dependence. That is, the probability of detection as a function of angle is 100 percent in Koopman's original derivation.

In the case of more than one AUV, the same formula can be used with the exception that the power in the exponential term must be multiplied by the number of AUVs. The reason for this is simple: Each AUV conducts a random search, which means that the motions of multiple AUVs are completely independent. Thus, using two AUVs, for instance, is equivalent to having one AUV execute a random search for twice the search time. In general, then, the probability of detection by *a* identical AUVs can be expressed as:

$$P_K(a) = 1 - e^{-\left(\frac{2 \cdot a \cdot \lambda_r \cdot V \cdot t}{A} \cdot \frac{\lambda_\theta}{\pi}\right)} \tag{12}$$

## MINE COUNTERMEASURES EXPLORATORY OPERATIONS

This experiment is intended to test concepts of MCM exploratory operations. The search area is divided into a total of *N* cells. Each cell is a square, has the same size, and contains at most one mine. For simplicity's sake, we assume that there is a uniformly random probability of having *n* mines in the search area, where *n* ranges from zero to *N;* that is, $p(n) = 1/N$. This choice is arbitrary and can be replaced by any other density distribution; it does not affect the derivation below. These *n* mines are further distributed randomly among the *N* cells. The experiment's objective is to determine the resources required to establish the presence or absence of mines in the search area.

Resources are measured in terms of the number of cells that are fathomed, denoted by *m*. When searching *m* cells, there is a probability that $m_d$ of these cells have mines and the remaining $m_a = m - m_d$ have no mines. The probability associated with such an event belongs to a hypergeometric density distribution:

$$P_{m_d, m_a} = \frac{\binom{n}{m_d} \cdot \binom{N-n}{m_a}}{\binom{N}{m = m_d + m_a}} \tag{13}$$

There are two possible outcomes from a search in a cell with a mine: detected or not detected. Assuming there is a mine, we will denote the probability of detection with $P_d$ and the probability of non-detection with $Q_d$, where *d* stands for detection. There are also two possible outcomes from a search in a cell with no mines: false alarm and no false alarm. Assuming there is no mine, we will denote the probability of a false alarm with $P_a$ and the probability of no false alarm with $Q_a$, where *a* stands for alarm. Combining the detection probability and the false-alarm probability of each cell with the hypergeometric density distribution, we obtain the probability of finding at least one object that looks like a mine:

$$P_e = \frac{1}{N} \cdot \sum_{n=0}^{N} \left( 1 - \sum_{m_d + m_a = m} P_{m_d, m_a} \cdot (Q_d)^{m_d} \cdot (Q_a)^{m_a} \right) \tag{14}$$

As this is a first attempt to analyze exploratory operations, we have picked an area where the environment is benign; that is, where $Q_a = 1$. In this scenario, then, the probability of finding at least one mine is equal to:

$$P_e = \frac{1}{N} \cdot \sum_{n=0}^{N} \left( 1 - \sum_{m_d + m_a = m} P_{m_d, m_a} \cdot (1 - P_d)^{m_d} \right) \tag{15}$$

## NUMERICAL RESULTS

Fig. 7 shows the probabilities of detecting at least one mine as a function of the number of searched cells. We pick the same search time, 6 hours, for each cell and for each search pattern. The inputs to determine the probabilities of detection are shown in Appendix B. We assume that there is at most one mine in each cell.

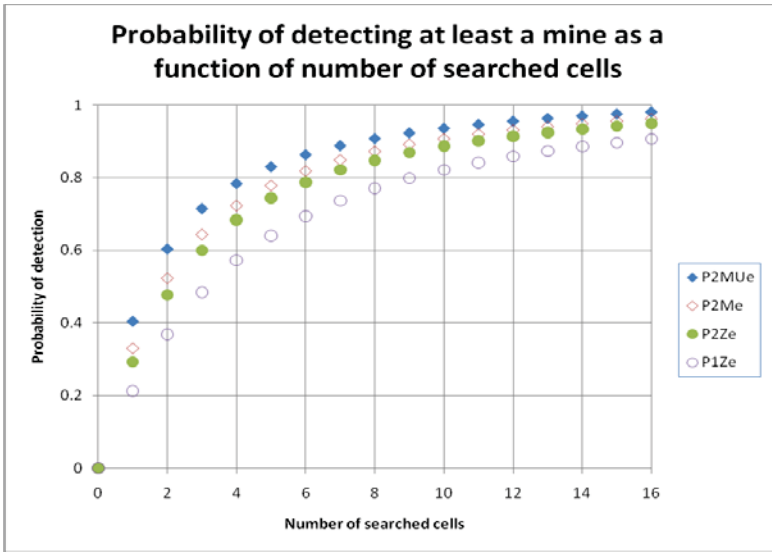


Figure 7. Probability of detecting at least one mine vs. number of searched cells.

Table 3 – Probability of detection for a search time of 6 hours.

| Search Pattern | 2M | 2MU | 2Z | 1Z | 2K | 1K |
|---|---|---|---|---|---|---|
| Probability of Detection | 0.62 | 0.76 | 0.55 | 0.40 | 0.69 | 0.45 |

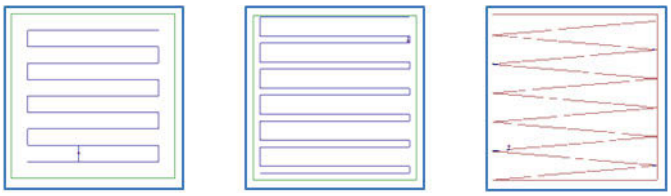

Figure 8a. Searched with one AUV – even lawn-mowing pattern (LHS), uneven lawn-mowing pattern (middle) and zigzag pattern (RHS).

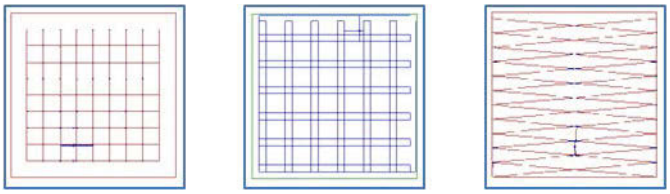

Figure 8b. Search with two AUVs – even lawn-mowing patterns (LHS), uneven lawn-mowing patterns (middle) and zigzag patterns (RHS).

Fig. 8a shows three different search patterns for one AUV. Fig. 8b shows three different hatching search patterns for two AUVs. The search patterns in Fig. 8a are variants of the lawn mowing pattern while the search patterns in Fig. 8b are simple extensions of those in Fig. 8a. Note that Fig. 8a and Fig. 8b are not drawn to scale. They are meant for illustrating the patterns only.

P2Me (e for exploratory operations) corresponds to two perpendicular, regular lawn-mowing patterns 2M, as shown on the LHS of Fig. 8b; P2MUe corresponds to two perpendicular, uneven lawn-mowing patterns 2MU, as shown in the middle of Fig. 8b; P2Ze corresponds to two complementary zigzag patterns 2Z, as shown on the RHS of Fig. 8b; and P2Ke corresponds to random search patterns 2K conducted by two AUVs. For completeness, Fig. 8a also illustrates patterns conducted by one AUV. The values of the probabilities of detection for the search patterns 2M, 2MU etc are displayed in Table 3.

Fig. 7 shows that P2MUe is the best among the four scenarios. This improvement is most significant for numbers of searched cells less than six ($m \le 6$). Such an improvement helps reduce resource and time requirements when conducting MCM operations. For instance, a 2Z search pattern takes at least 36 hours (searching 6 cells) to achieve the same probability of detecting at least one mine as a 2MU pattern that takes 24 hours (searching 4 cells). Equivalently, the probability of detecting at least one mine after searching 4 cells using the 2MU search pattern is more than 10 percent higher than that achieved using the 2Z search pattern – a substantial improvement in the confidence of finding at least one mine. This shows the importance of choosing the right search pattern.

In an effort to keep this paper to a reasonable length, we will discuss non-uniform mine density distributions in a future paper.

## Non-Uniform Mine Density Distributions

While the choice is clear in the case of a uniform mine density distribution, as described above, it is less obvious in the case of a non-uniform density distribution. Below, we make use of a derivation to analyze an exponential mine density distribution along the *y* (vertical) axis. This technique can be used to derive the optimal AUV path in general, assuming an *a priori* mine density distribution in the search area. To simplify the mathematics, we look for the AUV path as a line, rather than as an area, that maximizes the probability of detection. The optimal path is a solution to the Euler equation for $W\left[y(x)\right]$ in the search area, which can be expressed as:

$$W\left[y(x)\right] = \int_{\Delta x}^{X-\Delta x} dx \cdot \sqrt{1+\left(\frac{dy}{dx}\right)^2} \cdot f(x) \cdot g(y) \tag{16}$$

where $\Delta x$ is the margin on the left and the right of the AUV path. As an example, we assume $f(x)$ is the uniform density distribution along *x:*

$$f(x) = \begin{cases} 1/X \ if \ 0 \le x \le X \\ 0 \ otherwise \end{cases} \tag{17}$$

while $g(y)$ is the exponential density distribution along *y:*

$$g(y)=\begin{cases}\dfrac{e^{-|y-Y/2|/b}}{2\cdot b\cdot\left(1-e^{-Y/(2\cdot b)}\right)} & if\ 0\le y\le Y\\ 0 & otherwise\end{cases} \tag{18}$$

As illustrated in Fig. 9, it is typical in search operations to divide the search area into sub-box areas (such as the shaded rectangular area) when the AUV employs the lawn-mowing pattern. The figure shows the AUV path in the sub-box area within the ellipse. Note that the AUV's starting point is the dot at the lower left and its ending point is the dot at the upper right. We will answer the following question: Given a sub-box area like the one just described, what is the optimal path starting from the lower left dot and ending at the upper right dot?

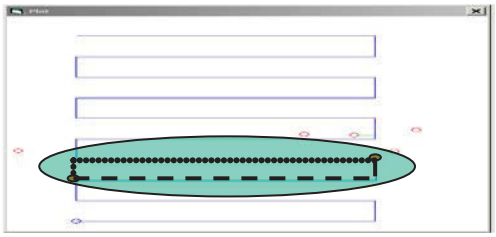

Figure 9. Optimal path (dotted) in a sub-box area.

Substituting the density distributions $f(x)$ and $g(y)$ into Eq. (19), and assuming that $y(x)$ is monotonically increasing, we get:

$$\begin{aligned}W &\le \int_{\Delta x}^{X-\Delta x}\frac{dx}{X}\cdot\left(1+\frac{dy}{dx}\right)\cdot\frac{e^{-(Y/2-y)/b}}{2\cdot b\cdot\left(1-e^{-Y/(2\cdot b)}\right)}\\ &\le \int_{\Delta x}^{X-\Delta x}\frac{dx}{X}\cdot\frac{e^{-(Y/2-y)/b}}{2\cdot b\cdot\left(1-e^{-Y/(2\cdot b)}\right)}+\int_{y_s}^{y_g}\frac{dy}{X}\cdot\frac{e^{-(Y/2-y)/b}}{2\cdot b\cdot\left(1-e^{-Y/(2\cdot b)}\right)}\\ &\le P_X+P_Y\end{aligned} \tag{20}$$

where $y_s$ is the starting $y$ coordinate of the AUV path and $y_e$ is the ending $y$ coordinate.

$$P_X = \int_{\Delta x}^{X-\Delta x} \frac{dx}{X} \cdot \frac{e^{-(Y/2-y)/b}}{2 \cdot b \cdot \left(1 - e^{-Y/(2 \cdot b)}\right)}; \; P_Y = \int_{y_s}^{y_e} \frac{dy}{X} \cdot \frac{e^{-(Y/2-y)/b}}{2 \cdot b \cdot \left(1 - e^{-Y/(2 \cdot b)}\right)} \tag{21}$$

Examining these expressions for $P_X$ and $P_Y$ closely, we realize that $P_X$ is the weight of the horizontal dotted line shown in Fig. 9, while $P_Y$ is the weight of the vertical dotted line. Since we have just demonstrated that the weight of any curve is less than the sum $P_X + P_Y$, this shows that the dotted line represents the optimal search path. This also confirms our intuition; that is, to optimize the weight of a search path, we need to let it be as close as possible to the half-width line, as this line corresponds to the highest mine density. Note that we obtain the same solution by solving Euler's equation through the functional expression of *W* (Gel'fand et al 1963).

We can also derive the optimal path for a more complex mine density distribution using the same formalism. For example, we can assume that both $f(x)$ and $g(y)$ are exponential distributions. That is, we replace the above definition of $f(x)$ in Eq. (12) by:

$$f(x) = \begin{cases} \dfrac{e^{-|x - X/2|/a}}{2 \cdot a \cdot \left(1 - e^{-X/(2 \cdot a)}\right)} & \text{if } 0 \le x \le X \\ 0 & \text{otherwise} \end{cases}$$

while $g(y)$ remains the same. The solution to the Euler-Lagrange equation is:

$$C \cdot e^{-\frac{1+\alpha^2}{a} \cdot x + \alpha \cdot z} = \left(-\sin(z) + \alpha \cdot \cos(z)\right)$$
$$z = \frac{1}{b} \cdot \left(x - \frac{y}{\alpha}\right) + D; \alpha = \frac{a}{b}$$

where $C$ and $D$ are constants that can be determined at the boundary conditions. We will further analyze this solution in a future paper.

## CONCLUSIONS

In this paper, we have examined a number of search patterns: lawn-mowing, zigzagging, and random searches. The measures of effectiveness of the first two patterns were evaluated through the use of a stochastic model and a deterministic one, whose outcomes were verified to be consistent.

Based on the assumed measures of performance, we demonstrated that the 2MU search pattern (two AUVs conducting perpendicular, uneven mowing patterns) provides the best probability of detection as a function of search time. This optimality is due to two features. First, the uneven mowing pattern is constructed so that there are no gaps between consecutive legs. Second, two perpendicular search patterns maximize the angular probability of detection, as proved in the main text and discussed in further detail in Appendix A.

We have also derived a novel result for an AUV conducting a random search while carrying a side-scan sonar. Although such an AUV cannot in reality collect data while employing a random search, it was useful to show that the 2MU search pattern achieves better effectiveness than a random search – a clue that 2MU is the right search pattern to use. The impact of search patterns on time and resource requirements for MCM exploratory operations was also determined.

In closing, we wish to note that all of the concepts of operations that this paper introduces can be implemented and tested in real-life scenarios, which might in fact be its true contribution.

## ACKNOWLEDGEMENTS

We are indebted to the reviewers for insightful comments and suggestions which help improve the quality of this paper.

## REFERENCES

Bays, M.J., A. Shende, D. J. Stilwell, and S.A. Redfield "A Solution to the Multiple Aspect Coverage Problem," International Conference on Robotics and Automation, Shanghai, China, 09-13 May 2011.

Couillard, M., J. Fawcett, M. Davison and V. Myers, "Optimizing time-limited multi-aspect classification", Proceedings of the Institute of Acoustics, 29 (6), pp. 89-96, 2007.

Fawcett, John A., Anna Crawford, David Hopkin, Vincent Myers and Benoit Zerr, "Computer-Aided Detection of Targets from the Citadel Trial Klein Sonar Data", Technical Memorandum TM 2006-115, November 2006.

Fawcett, John A., Anna Crawford, David Hopkin, Vincent Myers, Michel Couillard and Benoit Zerr, "Multi-Aspect Computer-Aided Classification of the Citadel Trial Sidescan Sonar Images", Technical Memorandum TM 2008-029, October 2008.

Gel'fand, I.M. and S.V. Fomin, *Calculus of Variations, 13th Edition,* Prentice-Hall, Englewood Cliffs NJ, U.S.A., 1964, p. 19.

Hill, R.R., R.G. Carl, and L.E. Champagne "Using Agent-Based Simulation To Empirically Examine Search Theory Using a Historical Case Study," Journal of Simulation 2006 (1), pp. 29-38.

Koopman, B.O. *Search and Screening: General Principles with Historical Applications,* Military Operations Research Society, Alexandria VA, U.S.A., 1999, pp. 71–74.

Law, Averill M. and W. David Kelton, *Simulation Modeling and Analysis, 3rd Edition,* McGraw-Hill, Boston MA, U.S.A., 2000, pp. 314–315.

Nguyen, B. and D. Hopkin, "Modeling Autonomous Underwater Vehicle (AUV) operations in mine hunting," Conference Proceedings of IEEE Oceans 2005 Europe, Brest, France, 20–23 June 2005a.

Nguyen, B. and D. Hopkin, "Concepts of Operations for the Side-Scan Sonar Autonomous Underwater Vehicles Developed at DRDC – Atlantic," Technical Memorandum TM 2005-213, October 2005b.

Nguyen, B., D. Hopkin, and H. Yip, "Autonomous Underwater Vehicles: A Transformation in Mine Counter-Measure Operations," Defense & Security Analysis 24 (3), 2008.

Press, W. H., S. A. Teukolsky, W. T. Vetterling and B. P. Flanney, Numerical Recipes in Fortran 77: The Art of Scientific Computing, Second Edition, Cambridge University Press, 1992, p. 295.

Quidu, I., J. Ph. Malkasse, P. Vilbé and G. Burel, "Mine Classification Based on a Multiview Characterisation", Undersea Defence Technology Europe Conference, Hamburg, Germany, 26-28 June 2001.

Vidyasagar, M. "Statistical Learning Theory and Randomised Algorithms for Control," IEEE Control System Magazine 18 (6), 1998, pp. 69–85.

Zerr, B., E. Bovio, and B. Stage, "Automatic mine classification approach based on AUV manoeuvrability and the COTS side scan sonar," Conference Proceedings of Autonomous Underwater Vehicle and Ocean Modelling Networks: GOAT2 2000, 2000, pp. 315–322.

Zwillinger, Daniel (editor), *CRC Standard Mathematical Tables and Formulae, 30th Edition,* CRC Press, Boca Raton FL, U.S.A., 1996, p. 608 and p. 333.

## APPENDIX A – OPTIMAL OBSERVATION ANGLE BETWEEN TWO AUV LEGS

In the main text, we have shown that the mean angular probability of detection, $P_2(\phi)$, generated by two AUV legs achieves an optimum when the angle $\phi$ between the two legs

is equal to $\phi = 90\ \text{deg}\left(\frac{\pi}{2}\right)$. This appendix further shows that this value is in fact a global maximum. It is true because of the shape and symmetry of the angular probability of detection with respect to $\phi = 90\ \text{deg}\left(\frac{\pi}{2}\right)$.

For the purpose of this appendix, it is convenient to redefine the aspect angle $\theta$ by shifting it to the left by $\phi = 90\ \text{deg}\left(\frac{\pi}{2}\right)$ such that the maximum angular probability of detection occurs at $0\ \text{deg}(0)$. There are many ways to prove that $P_2\left(\phi = \frac{\pi}{2}\right)$ is a global maximum. We choose to show that $P_2\left(\phi = \frac{\pi}{2}\right) > P_2\left(\phi = \frac{\pi}{2} + \varphi\right)$ for any $\varphi$. However, due to the periodicity of $f(\theta)$, it is sufficient to show that this is true for all $\varphi$ between $0\ \text{deg}(0)$ and $\phi = 90\ \text{deg}\left(\frac{\pi}{2}\right)$.

Recall that $P_2(\phi)$ is defined as:

$$P_2(\phi) = 1 - \frac{1}{\pi} \cdot \int_{-\frac{\pi}{2}}^{\frac{\pi}{2}} d\theta \cdot \left(1 - f(\theta)\right) \cdot \left(1 - f(\theta + \phi)\right) \tag{22}$$

Hence:

$$P_2\left(\frac{\pi}{2} + \varphi\right) = 1 - \frac{1}{\pi} \cdot \int_{-\frac{\pi}{2}}^{\frac{\pi}{2}} d\theta \cdot \left(1 - f(\theta)\right) \cdot \left(1 - f\left(\theta + \frac{\pi}{2} + \varphi\right)\right) \tag{23}$$

Since $f(\theta)$ is a periodic function with a period of 180 deg$(\pi)$:

$$\begin{aligned} P_2\left(\frac{\pi}{2}+\varphi\right) &= 1-\frac{1}{\pi}\cdot\int_{-\frac{\pi}{2}}^{\frac{\pi}{2}} d\theta\cdot\left(1-f(\theta)-f\left(\theta+\frac{\pi}{2}+\varphi\right)+f(\theta)\cdot f\left(\theta+\frac{\pi}{2}+\varphi\right)\right) \\ &= \frac{2\cdot\lambda_\theta}{\pi}-\frac{1}{\pi}\cdot\int_{-\frac{\pi}{2}}^{\frac{\pi}{2}} d\theta\cdot f(\theta)\cdot f\left(\theta+\frac{\pi}{2}+\varphi\right) \end{aligned} \tag{24}$$

where $\lambda_\theta$ is the scale compounded to Johnson's curve as defined in the main text. Thus, showing that $P_2\left(\phi=\frac{\pi}{2}\right)$ is a maximum is equivalent to showing that $\int_{-\frac{\pi}{2}}^{\frac{\pi}{2}} d\theta\cdot f(\theta)\cdot f\left(\theta+\frac{\pi}{2}\right)$ is a minimum, in the sense that:

$$\int_{-\frac{\pi}{2}}^{\frac{\pi}{2}} d\theta\cdot f(\theta)\cdot f\left(\theta+\frac{\pi}{2}+\varphi\right) \geq \int_{-\frac{\pi}{2}}^{\frac{\pi}{2}} d\theta\cdot f(\theta)\cdot f\left(\theta+\frac{\pi}{2}\right) \tag{25}$$

Rewrite the left-hand side as follows:

$$\begin{aligned} \int_{-\frac{\pi}{2}}^{\frac{\pi}{2}} d\theta\cdot f(\theta)\cdot f\left(\theta+\frac{\pi}{2}+\varphi\right) &= \int_{-\frac{\pi}{2}}^{0} d\theta\cdot f(\theta)\cdot f\left(\theta+\frac{\pi}{2}+\varphi\right)+\int_{0}^{\frac{\pi}{2}} d\theta\cdot f(\theta)\cdot f\left(\theta+\frac{\pi}{2}+\varphi\right) \\ &= \int_{0}^{\frac{\pi}{2}} d\theta\cdot\left[f(\theta)\cdot f\left(\theta-\frac{\pi}{2}-\varphi\right)+f(\theta)\cdot f\left(\theta+\frac{\pi}{2}+\varphi\right)\right] \end{aligned} \tag{26}$$

Similarly, rewrite the right-hand side as:

$$\begin{aligned}\int_{-\frac{\pi}{2}}^{\frac{\pi}{2}} d\theta \cdot f(\theta) \cdot f\left(\theta+\frac{\pi}{2}\right) &= \int_{-\frac{\pi}{2}}^{0} d\theta \cdot f(\theta) \cdot f\left(\theta+\frac{\pi}{2}\right) + \int_{0}^{\frac{\pi}{2}} d\theta \cdot f(\theta) \cdot f\left(\theta+\frac{\pi}{2}\right) \\ &= \int_{0}^{\frac{\pi}{2}} d\theta \cdot \left[ f(\theta) \cdot f\left(\theta+\frac{\pi}{2}\right) + f(\theta) \cdot f\left(\theta-\frac{\pi}{2}\right) \right]\end{aligned} \tag{27}$$

Subtract the right-hand side from the left-hand side:

$$\begin{aligned}&A+B+C= \\ &\int_{0}^{\frac{\pi}{2}} d\theta \cdot f(\theta) \cdot \left( f\left(\theta-\frac{\pi}{2}-\varphi\right) - f\left(\theta-\frac{\pi}{2}\right) \right) + \int_{0}^{\frac{\pi}{2}} d\theta \cdot f(\theta) \cdot \left( f\left(\theta+\frac{\pi}{2}+\varphi\right) - f\left(\theta+\frac{\pi}{2}\right) \right)\end{aligned} \tag{28}$$

where:

$$A = \int_{\varphi}^{\frac{\pi}{2}} d\theta \cdot f(\theta) \cdot \left( f\left(\theta-\frac{\pi}{2}-\varphi\right) - f\left(\theta-\frac{\pi}{2}\right) \right) + \int_{0}^{\frac{\pi}{2}-\varphi} d\theta \cdot f(\theta) \cdot \left( f\left(\theta+\frac{\pi}{2}+\varphi\right) - f\left(\theta+\frac{\pi}{2}\right) \right) \tag{29}$$

$$B = \int_{0}^{\varphi} d\theta \cdot f(\theta) \cdot \left( f\left(\theta-\frac{\pi}{2}-\varphi\right) - f\left(\theta-\frac{\pi}{2}\right) \right) \tag{30}$$

$$C = \int_{\frac{\pi}{2}-\varphi}^{\frac{\pi}{2}} d\theta \cdot f(\theta) \cdot \left( f\left(\theta+\frac{\pi}{2}+\varphi\right) - f\left(\theta+\frac{\pi}{2}\right) \right) \tag{31}$$

To prove that $P_2\left(\phi=\frac{\pi}{2}\right)$ is a global maximum, we will show that $A, B, C \geq 0$. Note that we can remove the parameter $\lambda_\theta$ in the proof, as it is only a constant multiplied to Johnson's density distributions.

Proof for $A \geq 0$. Make a change of variable $\theta' = \theta + \varphi$ in the second integral, and use the knowledge that $f(\theta)$ is a periodic function with a period of 180 deg$(\pi)$:

$$
\begin{aligned}
A &= \int_{\varphi}^{\frac{\pi}{2}} d\theta \cdot f(\theta) \cdot \left( f\left(\theta - \frac{\pi}{2} - \varphi\right) - f\left(\theta - \frac{\pi}{2}\right)\right) + \int_{0}^{\frac{\pi}{2}-\varphi} d\theta \cdot f(\theta) \cdot \left( f\left(\theta + \frac{\pi}{2} + \varphi\right) - f\left(\theta + \frac{\pi}{2}\right)\right) \\
&= \int_{\varphi}^{\frac{\pi}{2}} d\theta \cdot f(\theta) \cdot \left( f\left(\theta - \frac{\pi}{2} - \varphi\right) - f\left(\theta - \frac{\pi}{2}\right)\right) + \int_{\varphi}^{\frac{\pi}{2}} d\theta \cdot f(\theta - \varphi) \cdot \left( f\left(\theta + \frac{\pi}{2}\right) - f\left(\theta + \frac{\pi}{2} - \varphi\right)\right) \\
&= \int_{\varphi}^{\frac{\pi}{2}} d\theta \cdot f(\theta) \cdot \left( f\left(\theta + \frac{\pi}{2} - \varphi\right) - f\left(\theta + \frac{\pi}{2}\right)\right) + \int_{\varphi}^{\frac{\pi}{2}} d\theta \cdot f(\theta - \varphi) \cdot \left( f\left(\theta + \frac{\pi}{2}\right) - f\left(\theta + \frac{\pi}{2} - \varphi\right)\right)
\end{aligned}
$$

Rewrite the integrand as a product:

$$
A = \int_{\varphi}^{\frac{\pi}{2}} d\theta \cdot \left( f(\theta - \varphi) - f(\theta)\right) \cdot \left( f\left(\theta + \frac{\pi}{2}\right) - f\left(\theta + \frac{\pi}{2} - \varphi\right)\right) \tag{32}
$$

Since $f(\theta)$ is monotonous for $\theta$ between *zero* deg$(0)$ and 90 deg$\left(\frac{\pi}{2}\right)$, the first term of the integrand is non-negative; i.e., $f(\theta - \varphi) - f(\theta) \geq 0$. Similarly, the second term of the integrand is also non-negative; i.e., $f\left(\theta + \frac{\pi}{2}\right) - f\left(\theta + \frac{\pi}{2} - \varphi\right) \geq 0$. Hence, the integrand of *A* is non-negative and thus *A* itself is non-negative.

Proof for $B \geq 0$. Rewrite $B$ as a sum of two integrals:

$$B = \int_0^{\frac{\varphi}{2}} d\theta \cdot f(\theta) \cdot \left( f\left(\theta - \frac{\pi}{2} - \varphi\right) - f\left(\theta - \frac{\pi}{2}\right)\right) + \int_{\frac{\varphi}{2}}^{\varphi} d\theta \cdot f(\theta) \cdot \left( f\left(\theta - \frac{\pi}{2} - \varphi\right) - f\left(\theta - \frac{\pi}{2}\right)\right)$$

Make a change of variable $\theta' = \varphi - \theta$ in the second integral:

$$B = \int_0^{\frac{\varphi}{2}} d\theta \cdot f(\theta) \cdot \left( f\left(\theta - \frac{\pi}{2} - \varphi\right) - f\left(\theta - \frac{\pi}{2}\right)\right) + \int_0^{\frac{\varphi}{2}} d\theta \cdot f(\theta - \varphi) \cdot \left( f\left(\theta - \frac{\pi}{2}\right) - f\left(\theta - \frac{\pi}{2} - \varphi\right)\right)$$

where we have used the even parity of $f(\theta)$ and its period of 180 deg$(\pi)$ in the second integral. Rewrite the sum of the two integrands as a product:

$$B = \int_0^{\frac{\varphi}{2}} d\theta \cdot \left(f(\theta) - f(\theta - \varphi)\right) \cdot \left( f\left(\theta - \frac{\pi}{2} - \varphi\right) - f\left(\theta - \frac{\pi}{2}\right)\right) \tag{33}$$

For $\theta \in \left[0, \frac{\varphi}{2}\right]$, the first term of the integrand is non-negative; i.e., $f(\theta) - f(\theta - \varphi) \geq 0$. Similarly, the second term of the integrand is non-negative; i.e., $f\left(\theta - \frac{\pi}{2} - \varphi\right) - f\left(\theta - \frac{\pi}{2}\right) \geq 0$. Hence, the integrand of $B$ is non-negative and thus $B$ itself is non-negative.

Proof for $C \geq 0$. The proof for $C \geq 0$ is identical to that for *B*.

Conclusion. Thus, we have shown that $A, B, C \geq 0$. Hence, $A + B + C \geq 0$. This confirms that $P_2\left(\phi = \frac{\pi}{2}\right)$ is a global maximum.

## APPENDIX B – PROBABILITIES OF DETECTION

In this Appendix, we provide the inputs that were used to determine the probabilities of detection in Table 3. The search area is a 3 km by 3 km square. The AUV speed is equal to 9 knots. The probabilities of detection as a function of range and as a function of angle are shown in Figure 4.

Search pattern 2M (even lawn mowing):

a. Spacing between consecutive and parallel legs is equal to 100 meters;
b. Offset from the boundary of the search area is equal to 100 meters;
c. Number of long and parallel legs is equal to 29 in each direction;
d. Turning time is equal to 1.25 minutes for each rotation of 90 degrees;
e. Total time (search time and turning time) is equal to 6 hours and 7 minutes;
f. Probability of detection is equal to 0.62.

The above spacing for search pattern 2M is chosen such that the total time is approximately 6 hours and the coverage is essentially one hundred percent if we do not account for the gaps in the detection performance.

Search pattern 2MU (uneven lawn mowing):

a. Small spacing between consecutive and parallel legs is equal to 63.5 meters;
b. Large spacing between consecutive and parallel legs is equal to 150.0 meters;
c. Offset from the boundary of the search area is equal to 63.5 meters;
d. Number of long and parallel legs is equal to 28 in each direction;
e. Turning time is equal to 1.25 minutes for each rotation of 90 degrees;
f. Total time (search time and turning time) is equal to 6 hours and 2 minutes;
g. Probability of detection is equal to 0.75.

As described in the main text, the 2MU large spacing is equal to $2 \cdot r_{\max} = 150$ meters and the small spacing is equal to $r_{\max} - r_{\min} = 63.5$ meters.

Search pattern 2Z (zigzag):

a. Zigzag angle between the horizontal axis and an AUV leg is equal to 2.0454 degrees;
b. Number of legs is equal to 28 in each direction;
c. Turning time is equal to 2.5 minutes for each u-turn;
d. Total time (search time and turning time) is equal to 6 hours and 5 minutes;
e. Probability of detection is equal to 0.55.

Search pattern 1Z (zigzag):

a. Zigzag angle between the horizontal axis and an AUV leg is equal to 2.0454 degrees;
b. Number of legs is equal to 28;
c. Turning time is equal to 2.5 minutes for each u-turn;
d. Total time (search time and turning time) is equal to 6 hours and 5 minutes;
e. Probability of detection is equal to 0.40.

Search pattern 2K and 1K (Koopman's random search):

a. Eqn (12): $P_K(a) = 1 - e^{-\left(\frac{2 \cdot a \cdot \lambda_r \cdot V \cdot t}{A} \cdot \frac{\lambda_\theta}{\pi}\right)}$;
b. $\lambda_r = 53.057$ meters;
c. $\lambda_\theta = 1.575$ radians;
d. $A = 9\,\text{km}^2$;
e. $V = 9$ knots;
f. $t = 6$ hours;
g. $\alpha = 2$ for 2K and $\alpha = 1$ for 1K;
h. Probability of detection is equal to 0.69 for 2K and 0.45 for 1K.